

Thermal Stability Analysis of Functionally Graded Sandwich Circular Plates of Variable Thickness

S.K. Jalali, M.H. Naei, A. Poorsolhjoui, *Member, IAENG*

Abstract—In the present study, the thermal stability of laminated functionally graded (FGM) circular plates of variable thickness subjected to uniform temperature rise based on the first-order shear deformation plate theory is presented. The laminated FGM plate with variable thickness is considered as a sandwich plate constituted of a homogeneous core of variable thickness and two constant thickness FGM face sheets whose material properties are assumed to be graded in the thickness direction according to a simple power law. In order to determine the distribution of the prebuckling thermal load along the radius, the membrane equation is solved using the shooting method. Subsequently, employing the pseudo-spectral method that makes use of Chebyshev polynomials, the stability equations are solved numerically to evaluate the critical temperature rise. The results demonstrate that the thermal stability is significantly influenced by the thickness variation profile, aspect ratio, the volume fraction index, and the core-to-face sheet thickness ratio.

Index Terms—FGM, pseudospectral method, thermal Stability, variable thickness plates

I. INTRODUCTION

Stability analysis and studies on the buckling behavior of plates have been always considered as one of the important subjects in structural analysis [1,2]. On the other hand, variable thickness plates have always been attractive for designers, and a lot of researches have been done on this subject. The most conspicuous usage of variable thickness plates is to lighten structures, especially when used in high-speed aircrafts. With an accurate design of the thickness distribution, one can make an increase in buckling capacity of the plate compared to its uniform thickness counterpart.

Functionally graded materials (FGM) are a group of composite materials whose properties vary continuously from one side to another. These materials are typically constructed from a mixture of ceramic and metal and they can survive environments with high-temperature gradients such as nuclear reactors and high-speed aircrafts. The low thermal conductivity of ceramic provides the high-temperature resistance. On the other hand, the ductile metal prevents fracture caused by thermal stresses. A huge number of

researches have done on the subject of buckling and post-buckling of FGM plates of constant thickness. However, the subject of FGM plates with variable thickness has been taken under advisement by researchers.

FGM plates would constitute a significant part of structural applications in future. On the other hand, optimum design is a big concern especially in applications such as aerospace, where reducing the structural members' weight is essential. Considering these facts demonstrates the importance of researches dealing with the behavior of FGM plates with variable thickness. However, with regard to the previous researches, it is obvious that the analysis of FGM plates with variable thickness, especially in the field of buckling problems, has not been noticed very much. Therefore, in this study, the thermal stability of FGM circular plates with variable thickness under radial compression is investigated for clamped and simply supported boundary conditions.

II. PROBLEM FORMULATIONS

A. Geometry

Consider a circular plate of radius b which is mid-plane symmetric, as shown in Fig. 1. The plate is under uniform temperature rise ΔT . The origin of the cylindrical coordinates system lies on the center of the mid-plane where r and z define the radial and thickness directions, φ defines the rotation about the radial axis, and u and w are the displacements in r and z directions, respectively. The plate studied here can be considered as a sandwich plate with a homogenous core of variable thickness, $h_H(r)$, and two FGM face sheets with constant thickness, h_f . Therefore, the overall thickness of the plate, $h(r)$, would be a function of r .

$$h_H(r) = h_{H1} + (h_{H2} - h_{H1}) \left(\frac{r}{b}\right)^p \quad (1)$$

$$h(r) = h_H(r) + 2h_f \quad (2)$$

where h_{1H} and h_{2H} are the thicknesses of the core at the center and the edge of the plate, respectively, and p defines the profile of the thickness. Although the formulation and the method are general for circular

plates with any kind of profile through the thickness, the analysis is performed only on plates with linear and parabolic profiles. The plate has three layers that the k^{th} layer is between z_k and z_{k+1} ($k=1, 2, \text{ and } 3$) coordinates.

$$z_1(r) = -\frac{h_H(r)}{2} - h_f \quad (3a)$$

$$z_2(r) = -\frac{h_H(r)}{2} \quad (3b)$$

$$z_3(r) = \frac{h_H(r)}{2} \quad (3c)$$

$$z_4(r) = \frac{h_H(r)}{2} + h_f \quad (3d)$$

Considering a plate of constant core volume, V_H , the relationship between the geometrical parameters is given by

$$h_{H0} = \frac{V_H}{\pi b^2} = h_{H1} + \frac{2(h_{H2} - h_{H1})}{p + 2} \quad (4a)$$

$$h_0 = h_{H0} + 2h_f \quad (4b)$$

$$\Omega = \frac{h_{H2}}{h_{H1} + h_{H2}} \quad (5)$$

where h_{H0} is the core thickness of its uniform thickness counterpart, and Ω is the taper parameter ranging from 0 to 1, defining the volume distribution of the core in radial direction.

Fig. 1. Geometrical definition of an FGM circular plate with variable thickness

B. FGM properties

The material properties of the FGM face sheets such as Young's modulus are functions of ceramic and metal volume fractions, V_c and V_m as follows

$$E_f = V_m E_m + V_c E_c \quad (6)$$

$$V_m = \left(\frac{z - z_1}{z_2 - z_1}\right)^N \quad z_1 \leq z \leq z_2 \quad (7a)$$

$$V_m = \left(\frac{z - z_4}{z_3 - z_4}\right)^N \quad z_3 \leq z \leq z_4 \quad (7b)$$

$$V_c = 1 - V_m \quad (7c)$$

where N is the volume fraction index ranging from 0 to ∞ .

C. Equilibrium and stability equations

In order to consider the nonlinear effects of the buckling problem, the axisymmetric strain-displacement relations are written based on von-Karman plate theory

$$\varepsilon_r = \varepsilon_{r0} + k_r z, \quad (8a)$$

$$\varepsilon_\theta = \varepsilon_{\theta 0} + k_\theta z, \quad (8b)$$

$$\gamma_{rz} = \varphi + w_{,r} \quad (8c)$$

in which the mid plane strains, ε_{r0} and $\varepsilon_{\theta 0}$, are given by

$$\varepsilon_{r0} = u_{,r} + \frac{1}{2}(w_{,r})^2, \quad \varepsilon_{\theta 0} = \frac{u}{r} \quad (9)$$

and the curvatures, k_r and k_θ are defined as

$$k_r = \varphi_{,r}, \quad k_\theta = \frac{\varphi}{r} \quad (10)$$

where $()_{,r}$ indicate the differentiation with respect to r .

The relations between stress and strain are based on Hook's law, while Poisson's ratio ν is assumed to be constant.

$$\sigma_r = \frac{E}{1 - \nu^2} (\varepsilon_r + \nu \varepsilon_\theta) - \frac{E\alpha\Delta T}{1 - \nu} \quad (11a)$$

$$\sigma_\theta = \frac{E}{1 - \nu^2} (\varepsilon_\theta + \nu \varepsilon_r) - \frac{E\alpha\Delta T}{1 - \nu} \quad (11b)$$

$$\tau_{rz} = \frac{E}{2(1 + \nu)} \gamma_{rz} \quad (11c)$$

The resultant forces and moments of the stresses are given by

$$(N_r, N_\theta) = \int_{-h(r)/2}^{h(r)/2} (\sigma_r, \sigma_\theta) dz \quad (12a)$$

$$(M_r, M_\theta) = \int_{-h(r)/2}^{h(r)/2} (\sigma_r, \sigma_\theta) z dz \quad (12b)$$

$$Q_r = K \int_{-h(r)/2}^{h(r)/2} \tau_{rz} dz \quad (12c)$$

where K is the shear correction coefficient in the first-order shear deformation plate theory, which is set to $5/6$. Substituting Eq. (11) into Eq. (12) results in the following relations between resultant forces and moments and the strains.

$$\begin{pmatrix} N_r \\ N_\theta \end{pmatrix} = A_{11} \begin{bmatrix} 1 & \nu \\ \nu & 1 \end{bmatrix} \begin{pmatrix} \varepsilon_{r0} \\ \varepsilon_{\theta 0} \end{pmatrix} - \begin{pmatrix} N_r^T \\ N_\theta^T \end{pmatrix} \quad (13a)$$

$$\begin{pmatrix} M_r \\ M_\theta \end{pmatrix} = D_{11} \begin{bmatrix} 1 & \nu \\ \nu & 1 \end{bmatrix} \begin{pmatrix} k_r \\ k_\theta \end{pmatrix} - \begin{pmatrix} M_r^T \\ M_\theta^T \end{pmatrix} \quad (13b)$$

$$Q_r = A_{55} \gamma_{rz} \quad (13c)$$

$$(A_{11}, D_{11}) = \int_{-h(r)/2}^{h(r)/2} (1, z^2) \frac{E(z)}{1 - \nu^2} dz \quad (14a)$$

$$A_{55} = \frac{KA_{11}(1-\nu)}{2} \quad (14b)$$

The thermal membrane forces N_r^T and N_θ^T and thermal bending moments M_r^T and M_θ^T are calculated by

$$(N_r^T, M_r^T) = \int_{-h(r)/2}^{h(r)/2} \frac{E(z)}{1-\nu} \alpha(z) \Delta T(1, z) dz \quad (15a)$$

$$(N_\theta^T, M_\theta^T) = (N_r^T, M_r^T) \quad (15b)$$

Equilibrium equations of the circular plate with axisymmetric deformations can be obtained by using stationary potential energy method as follows

$$N_{r,r} + \frac{N_r - N_\theta}{r} = 0 \quad (16a)$$

$$Q_r + rQ_{r,r} + (rN_r w_{,r})_{,r} = 0 \quad (16b)$$

$$M_{r,r} + \frac{M_r - M_\theta}{r} - Q_r = 0 \quad (16c)$$

Substituting Eqs. (8)-(10) and (13) into Eq. (16) gives the equilibrium equations in terms of the displacement components.

$$A_{11}w_{,r}w_{,rr} + \frac{1}{2r}[A_{11}(1-\nu) + rA_{11,r}]w_{,r}^2 + A_{11}u_{,rr} + \frac{1}{r}(A_{11} + rA_{11,r})u_{,r} + \frac{1}{r}\left(\nu A_{11,r} - \frac{A_{11}}{r}\right)u - N_{r,r}^T = 0 \quad (17a)$$

$$w_{,rr}\{A_{55} + A_{11}\left[u_{,r} + \frac{3}{2}(w_{,r})^2 + \nu \frac{u}{r}\right] - N_r^T\} + w_{,r}\{A_{55,r} + \frac{A_{55}}{r} + [\frac{A_{11}}{r}(1+\nu) + A_{11,r}]u_{,r} + \frac{1}{2r}(A_{11} + rA_{11,r})(w_{,r})^2 + \nu A_{11,r} \frac{u}{r} + A_{11}u_{,rr} - \frac{N_r^T}{r} - N_{r,r}^T\} + A_{55}\varphi_r + \left(A_{55,r} + \frac{A_{55}}{r}\right)\varphi = 0 \quad (17b)$$

$$D_{11}\varphi_{,rr} + \frac{1}{r}(D_{11} + rD_{11,r})\varphi_{,r} - \frac{1}{r}\left(\frac{D_{11}}{r} - \nu D_{11,r} + rA_{55}\right)\varphi - A_{55}w_{,r} - M_{r,r}^T = 0 \quad (17c)$$

One can obtain all the configurations of the plate from the above equation. There are two types of equilibrium configurations possible for a plate under in-plane loading, which are undeflected and buckled configurations. When buckling happens the plate configuration will turn from the undeflected configuration into the buckled one. The intersection of these two equilibrium configurations is called the bifurcation point. This point can be obtained by solution of linear differential equations of stability. The

linear equations of stability necessary for this process may be derived from the nonlinear equilibrium equations, Eq. (17), by use of a perturbation technique in which the displacement field, (u, w, φ) , is replaced by $(u_0 + u_1, w_0 + w_1, \varphi_0 + \varphi_1)$, where (u_0, w_0, φ_0) represents an equilibrium configuration in the undeflected state, and (u_1, w_1, φ_1) is a small increment. This method is called adjacent equilibrium criterion [2]. Therefore, the stability equations can be expressed as

$$A_{11}u_{1,rr} + \frac{1}{r}(A_{11} + rA_{11,r})u_{1,r} - \frac{1}{r^2}(A_{11} - \nu rA_{11,r})u_1 = 0 \quad (18a)$$

$$(A_{55} + N_{r0})w_{1,rr} + \frac{1}{r}[A_{55} + N_{r0} + r(A_{55,r} + N_{r0,r})]w_{1,r} + A_{55}\varphi_{1,r} + \frac{1}{r}(A_{55} + rA_{55,r})\varphi_1 = 0 \quad (18b)$$

$$D_{11}\varphi_{1,rr} + \frac{1}{r}(D_{11} + rD_{11,r})\varphi_{1,r} - \frac{1}{r^2}(D_{11} - \nu rD_{11,r} + r^2A_{55})\varphi_1 - A_{55}w_{1,r} = 0 \quad (18c)$$

The stability equations are homogenous and linear and have solutions only for discrete values of the applied load, which refers to an eigenvalue problem. The smallest eigenvalue is termed the critical buckling load P_{cr} . It should be noticed that Eq. (18a) is decoupled from the Eqs. (18b) and (18c). The boundary conditions for the stability equations are

$$\text{Center:} \quad \varphi_1 = 0, \quad w_{1,r} = 0 \quad (19a)$$

$$\text{Clamped:} \quad \varphi_1 = 0, \quad w_1 = 0; \quad (19b)$$

$$\text{Simply Supported:} \quad w_1 = 0, \quad \left(\varphi_{1,r} + \frac{\nu}{b}\varphi_1\right) = 0; \quad (19c)$$

In Eq. (18) N_{r0} is the prebuckling load, which must be obtained from the equilibrium equations of the plate. But since the plate is in its undeflected configuration, w_0 and φ_0 are equal to zero, and the equilibrium Eq. (17) can be revised into the following equation called the membrane equation.

$$A_{11}u_{0,rr} + \frac{1}{r}(A_{11} + rA_{11,r})u_{0,r} - \frac{1}{r^2}(A_{11} - \nu rA_{11,r})u_0 - N_{r0,r}^T = 0 \quad (20)$$

Solving the above equation, u_0 may be obtained and therefore, N_{r0} can be calculated from Eq. (13a). The boundary conditions for membrane equation can be expressed as

$$u_0 = 0 \quad \text{Center} \quad (21a)$$

$$u_0 = 0 \quad \text{Edge} \quad (21b)$$

The shooting method, consisting of the well known Runge-Kutta method in conjunction with a Newton-Raphson iterative formulation, is employed to numerically solve the membrane equation, Eq. (20).

III. NUMERICAL SOLUTION METHODS

The pseudospectral method is employed to numerically solve the eigenvalue problem, Eqs. (18) and (19). The basic idea in this method is to assume that the answer of the differential equations can be approximated by a sum of finite number of basis functions. Usually when the solution is not especially periodic, Chebyshev polynomials are the best choices as basis functions (from J. P. Boyd [3]). To approximate the answers with Chebyshev polynomials, the solution range should be changed from $r \in [0, b]$ to $x \in [-1, 1]$. The following dimensionless parameters are introduced to make the stability equations dimensionless

$$\begin{aligned} x_1 &= \frac{w_1}{b}, & x_2 &= \varphi_1, & \bar{N}_{r0} &= \frac{N_{r0}}{A_{55}}, \\ \bar{N}'_{r0} &= \frac{bN_{r0,r}}{2A_{55}}, & \bar{A}'_{55} &= \frac{bA_{55,r}}{2A_{55}}, & & \\ \bar{D}'_{11} &= \frac{bD_{11,r}}{2D_{11}}, & \bar{F} &= \frac{b^2A_{55}}{D_{11}} \end{aligned} \quad (22)$$

where x_1 and x_2 are dimensionless transverse displacement and rotation about the radial axis, respectively. Therefore, the stability equations, Eq. (18), and the boundary conditions, Eq. (19), can be rewritten in the following form, where ()' shows the derivative with respect to x .

$$\begin{aligned} &2(\bar{N}_{r0} + 1)x_1'' + \\ &2 \left[\frac{(\bar{N}_{r0} + 1)}{(x + 1)} + (\bar{A}'_{55} + \bar{N}_{r0}) \right] x_1' + x_2' \\ &+ \left[\frac{1}{(x + 1)} + \bar{A}'_{55} \right] x_2 = 0 \end{aligned} \quad (23a)$$

$$\begin{aligned} &2x_2'' + 2 \left[\frac{1}{(x + 1)} + \bar{D}'_{11} \right] x_2' \\ &- 2 \left[\frac{1}{(x + 1)^2} - \frac{\nu \bar{D}'_{11}}{(x + 1)} + \frac{\bar{F}}{4} \right] x_2 - \bar{F}x_1' = 0 \end{aligned} \quad (23b)$$

$$\text{Center} \quad x_1'(-1) = 0, \quad x_2(-1) = 0 \quad (24a)$$

$$\text{Clamped:} \quad x_1(1) = 0, \quad x_2(1) = 0 \quad (24b)$$

Simply Supported:

$$x_1(1) = 0, \quad \left(x_2'(1) + \frac{\nu}{2} x_2(1) \right) = 0 \quad (24c)$$

x_1 and x_2 are approximated by a sum of $n+1$ Chebyshev polynomials as follows

$$x_{1i} = \sum_{j=1}^{n+1} a_j T_{i,j} \quad (25a)$$

$$x_{2i} = \sum_{j=1}^{n+1} b_j T_{i,j} \quad (25b)$$

where indexes i and j refer to the i^{th} collocation point and the j^{th} Chebyshev polynomial, respectively, and a_j and b_j are unknown coefficients.

In order to solve the equations, $2n+2$ algebraic equations are needed. The boundary conditions, Eq. (24), provide four of the required equations. Besides, satisfying Eqs. (23a) and (23b) in $n-1$ collocation points supplies $2n-2$ remained algebraic equations. To minimize the error, based on the Gauss-Lobatto interpolation points, the optimal collocation points can be selected as follows.

$$x_i = \cos\left(\frac{\pi i}{N-2}\right) \quad i = 0, 1, 2, \dots, N-2 \quad (26)$$

The results are represented in dimensionless form using the buckling load factor λ defined by

$$\lambda_T = 12(1 + \nu_f) \Delta T_{cr} \alpha_c \left(\frac{b}{h_0}\right)^2 \quad (27)$$

IV. NUMERICAL RESULTS AND DISCUSSIONS

A. Homogenous plates

Since there are no results submitted for the problem being studied, the problem is solved for a homogenous plate in order to validate the present study, and for this purpose h_f is considered to be equal to zero.

For the purpose of verifying the buckling behavior, a comparison study for thick circular plates with constant thickness is made with those obtained by Wang et al. [4] using Rayleigh-Ritz energy approach, Raju and Rao [5] using Galerkin's method, and Özakça [6] applying FEM in Table 1.

Table 1. Comparisons of the present buckling load factors λ

Reference	h_0/b				
	0.001	0.05	0.1	0.2	
C	Present	14.6819	14.5296	14.0909	12.5724
	[4]	14.6819	14.5296	14.0909	12.5725
	[5]	14.6825	14.5299	14.0910	12.5725
	[6]	14.6819	14.5014	13.9885	12.2843
	[1]	14.6842	14.6842	14.6842	14.6842
SS	Present	4.1978	4.1852	4.1480	4.0056
	[4]	4.1978	4.1853	4.1480	4.0056
	[5]	4.1978	4.1852	4.1481	4.0056
	[6]	4.1978	4.1844	4.1448	3.9938
	[1]	4.2025	4.2025	4.2025	4.2025

B. FGM plates

In this section, the results of thermal stability analysis of variable thickness FGM circular plates under radial compression are presented. The FGM face sheets are made from a mixture of aluminum (*Al*) and zirconia (*ZrO₂*) whose properties are summarized in Table 2 and the homogenous core is also made of aluminum. Poisson's ratio is considered to be constant and equal to 0.3.

Table 2. Material properties of aluminum and zirconia in the FGM face sheets from Praveen and Reddy [7]

Materials	Young's modulus (GPa)	Thermal expansion coefficient (1/°C)
Aluminum	70	23×10 ⁻⁶
Zirconia	151	10×10 ⁻⁶

Fig. 2 displays the variations of the buckling factor λ_T with the volume fraction index N for specified values of h_{H0}/h_f . The results are presented for a plate with constant core thickness ($\Omega=0.5$) and aspect ratio $h_0/b=0.06$. It can be seen that as the volume fraction index N is increased, the buckling factor λ_T increases. The reason is that an increase in the volume fraction index N results in an increase in the volume fraction of ceramic; and as the thermal expansion of ceramic is lower than metal, the plate's resistance to the buckling increases. Increase in the volume fraction of ceramic is possible with both increase in the volume fraction index N and decrease in the core-to-face sheet thickness ratio h_{H0}/h_f . Increasing the volume fraction index N in the approximate range of 0 to 5 causes significant increase in the buckling load factor λ_T , and after that it varies slowly until the plate becomes almost ceramic. From Fig. 2 it can be observed that, for a specified value of N , the maximum value of the buckling factor λ_T corresponds to $h_{H0}/h_f=0$, which refers to a plate without a homogenous core. On the contrary, a plate with thin FGM face sheets ($h_{H0}/h_f=10$) has the minimum value of the buckling factor.

In order to investigate the effect of the volume fraction on the buckling behavior from another point of view, variations of the buckling load factor λ_T with the core-to-face sheet thickness ratio h_{H0}/h_f for specified values of the volume fraction index N for a plate with constant core thickness ($\Omega=0.5$) and aspect ratio of $h_0/b=0.06$ is displayed in Fig. 3. The maximum buckling factor λ_T corresponds to $N=100$ and $h_{H0}/h_f=0$ that refers to a plate without a homogenous core and with almost ceramic face sheets and the lowest one corresponds to $N=0$, which refers to a plate with fully metal face sheets. It is obvious that when $N=0$, the plate is fully metal and variations of the ratio h_{H0}/h_f is of no effect on the buckling factor λ_T .

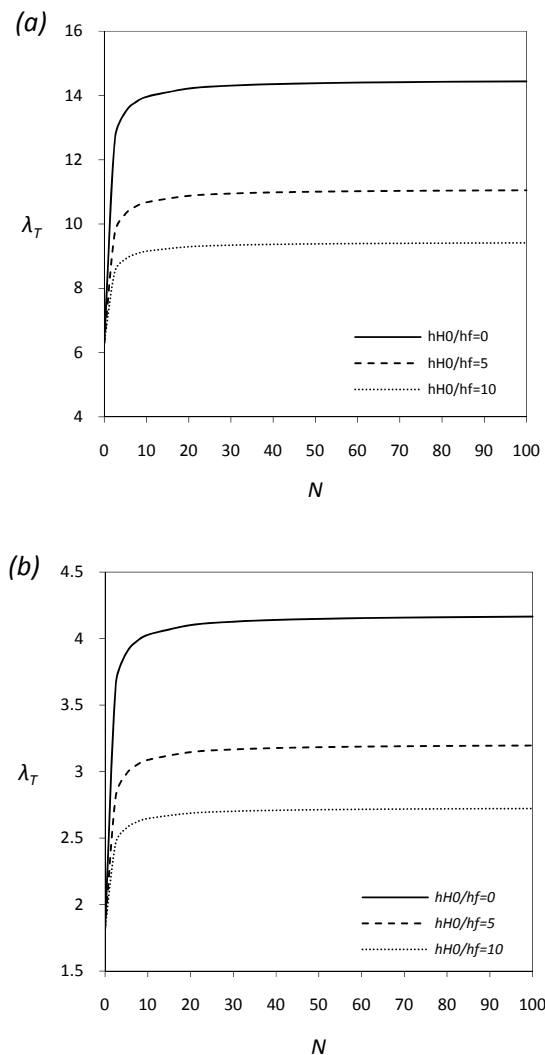


Fig. 2. Relationship between the buckling load factor λ_T and the volume fraction index N for specified values of core-to-face sheet thickness ratio h_{H0}/h_f . (a) Clamped edge (b) Simply supported edge.

V. CONCLUSION

The thermal stability of laminated FGM circular plates with variable thickness under radial compression based on the first-order shear deformation plate theory and nonlinear von-Karman displacement field is studied. Numerical solution for both clamped and simply supported boundary conditions and for either linear or parabolic taper is presented. Since there are no results submitted for the problem being studied, for the purpose of verifying the accuracy of the results, the critical temperature rise for homogenous plates is compared with the previous researches. The comparison shows that the results derived using the current method compare very well with them.

Because variation in the volume fraction of ceramic and metal is possible with both variations in the volume fraction index N and the core-to-face sheet thickness ratio h_{H0}/h_f , the effect of these two parameters on the buckling behavior is investigated. Increasing the volume fraction index N and decreasing the core-to-face sheet thickness ratio h_{H0}/h_f both result in increase in the volume fraction of ceramic in the plate and therefore, increase in the buckling load factor λ_T .

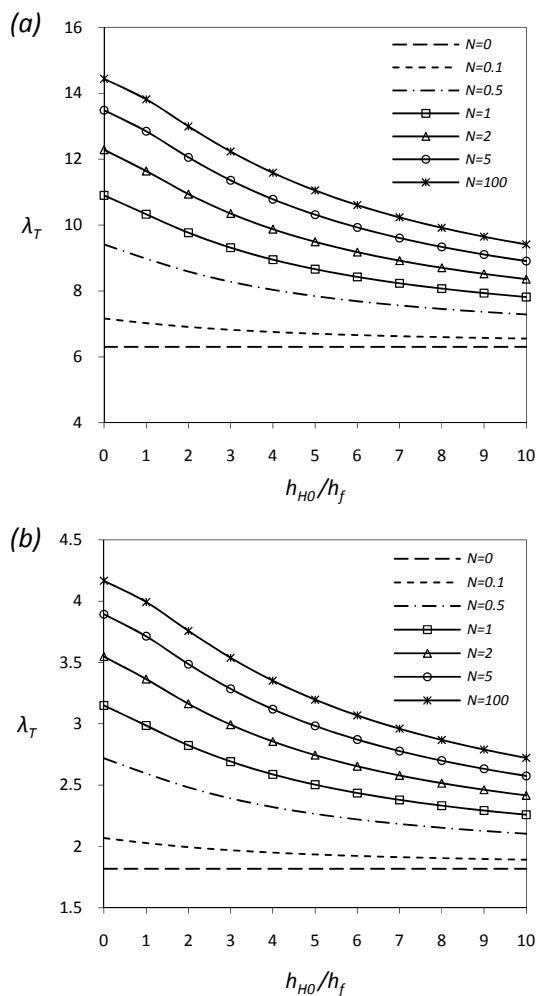


Fig. 3. Buckling load factor λ_T with respect to the core-to-face sheet thickness ratio h_{H0}/h_f for specified values of the volume fraction index N . (a) Clamped edge (b) Simply supported edge

REFERENCES

- [1] S. P. Timoshenko, and J. M. Gere, Theory of elastic stability. 2nd ed. New York: McGraw-Hill; 1961.
- [2] D. O. Brush, and B. O. Almroth, Buckling of Bars, Plates and Shells. New York: McGraw-Hill; 1975.
- [3] J. P. Boyd, Chebyshev and Fourier Spectral Methods. New York: Dover; 2000.
- [4] K. K. Raju, and G. V. Rao, Thermal post-buckling of linearly tapered moderately thick isotropic circular plates. Comput Struct 1996;58:655-8.
- [5] C. M. Wang, Y. Xiang, S. Kitipornchai, and K. M. Liew, Axisymmetric buckling of circular Mindlin plates with ring supports. J Struct Eng 1993;119:782-93.
- [6] M. Özakça, N. Taysi, and F. Kolcu, Buckling analysis and shape optimization of elastic variable thickness circular and annular plates—I. Finite element formulation. Eng Struct 2003;25:181-92.
- [7] Praveen GN, Reddy JN. Nonlinear transient thermoelastic analysis of functionally graded ceramicmetal plates. Int J Solids Struct 1998;33:4457-76.